Journal of ELECTRONIC MATERIALS, Vol. 43, No. 4, 2014
DOI: 10.1007/s11664-014-3005-9

The Effect of Growth Pressure and Growth Rate on the Properties of Mg-Doped GaN

BINGLEI FU,[1,2] NAIXIN LIU,[1] NING ZHANG,[1] ZHAO SI,[1] XUECHENG WEI,[1] XIAODONG WANG,[1] HONGXI LU,[1] ZHE LIU,[1] TONGBO WEI,[1] XIAOYAN YI,[1] JINMIN LI,[1] and JUNXI WANG[1]

1.—Research and Development Center for Semiconductor Lighting, Chinese Academy of Sciences, P.O. Box 912, Beijing 100083, People's Republic of China. 2.—e-mail: fubinglei@semi.ac.cn

In this work, the effects of growth pressure and growth rate on electrical and structural properties of Mg-doped GaN were investigated. It has been shown that enhanced growth rates induced by higher growth pressures may lead to decreased structural and electrical properties of *p*-type GaN layers. If the growth rate is kept unchanged, higher growth pressures will be beneficial for the quality of Mg-doped GaN due to the enhanced NH_3 overpressure.

Key words: *p*-GaN, Mg doping, adatom surface mobility, Mg incorporation ability, growth rate, growth pressure, MOCVD, GaN

INTRODUCTION

Recently, GaN-based light-emitting diodes (LEDs) have attracted considerable attention and great progress has been made in this area. However, the situation is far from satisfactory. One of the key problems is the poor quality of the *p*-type GaN layer, which may lead to low hole concentration and relatively high turn-on voltage of the device. Many new techniques have been designed to solve this problem, including *p*-InGaN,[1,2] delta doping,[3–5] *p*-GaN superlattices,[6,7] etc. Moreover, there are also many works focusing on the growth conditions of *p*-GaN layers, such as temperature, Mg concentration, carrier gas, V/III ratio, and growth rate and pressure.[8–11] However, some factors do not act separately. For some kinds of metalorganic chemical vapor deposition (MOCVD) reactors, the growth pressure has a great influence on the growth rate. As far as we know, very few works have focused on the joint influence of these factors.[12] Therefore, a comprehensive study on the influence of growth pressure and growth rate on the properties of *p*-GaN is necessary.

In this work, we focused on the reactor pressure region where growth rates change dramatically with growth pressure and examined the joint effect of some closely related growth parameters such as growth rate, pressure, and V/III ratio on the electrical and structural properties of Mg-doped GaN.

(Received August 30, 2013; accepted January 3, 2014; published online January 22, 2014)

EXPERIMENTAL PROCEDURES

Mg-doped *p*-GaN layers were grown with a Veeco P125 metalorganic chemical vapor deposition (MOCVD) system (Veeco Instruments, Inc., New York, USA). Trimethylgallium (TMGa) and ammonia were used as group III source and group V source separately, whereas biscyclopentadienyl magnesium (Cp_2Mg) was used as *p*-type dopant and hydrogen (H_2) as the carrier gas during *p*-GaN layer growth. *p*-Type GaN samples were grown directly on preprepared undoped GaN layers to avoid the influence of the nucleation layer and undoped layer on the properties of the *p*-type layer. Our undoped GaN layers were grown in a single run with a homemade 7 × 2 inch MOCVD system to keep their properties uniform. Substrates were cleaned in H_2 at 1085°C, then a 25-nm low-temperature (LT) GaN nucleation layer was deposited on the substrate at 520°C, followed by a 2-μm-thick undoped GaN layer grown at 1050°C. Then, the 500-nm *p*-type layers were grown on these undoped GaN layers in the Veeco P125 system. The growth temperature of *p*-type GaN was 950°C. The growth pressure was varied from 130 Torr to 650 Torr. In sample series I, the growth pressure was the only varying parameter, whereas the unchanged V/III ratio was

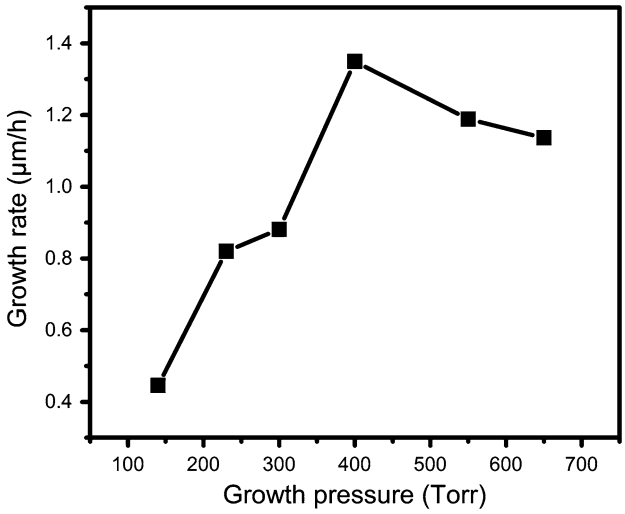

Fig. 1. Dependence of *p*-GaN growth rate and Mg concentration on growth pressure at fixed V/III ratio of 5000 and Cp_2Mg/TMGa ratio of 0.3%.

5000. In sample series II, the Ga and Mg flow rates were reduced to keep a constant growth rate when the growth pressure increased; as a result, the V/III ratio varied from 5000 to 16,000. All of the samples were grown at constant Cp_2Mg/TMGa ratio of 0.3%.

All samples were annealed for 10 min at 720°C in the MOCVD reactor to activate the dopants. The growth rates of the *p*-GaN layers were calibrated *in situ* by optical reflectivity measurements. Standard 7 mm × 7 mm square samples were made for Hall-effect measurements in van der Pauw geometry at room temperature to examine the electrical properties of the *p*-type GaN layers. Atomic force microscopy (AFM) scans were performed to observe the surface morphologies of samples using a Nanoscope Dimension™ 3100 (Veeco Instruments, Inc., New York, USA) scanning probe microscope system. The Mg concentrations of our samples were determined by secondary-ion mass spectrometry (SIMS). The optical properties of our samples were examined by room-temperature (RT) photoluminescence (PL) measurements using a 325-nm laser excitation source.

RESULTS AND DISCUSSION

Figure 1 shows the dependence of the *p*-GaN layer growth rate on the growth pressure. The growth rate increased significantly from 130 Torr to 400 Torr, and then slowly decreased under higher growth pressure. It is known that, in ideal Turbo-Disk reactors under the growth conditions used in our experiment, the growth rate is mainly controlled by the mass transport of reactant through the boundary layer and should be proportional to the square root of the reactor pressure.[13,14] However, the growth rate increased almost linearly from 130 Torr to 400 Torr in our experiment, which may be caused by the nonideality of our reactor. The

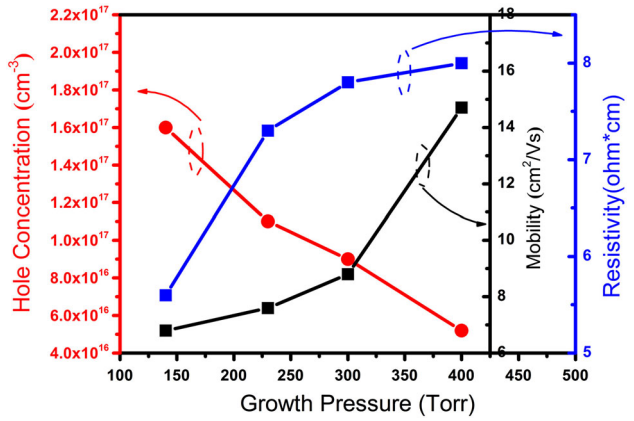

Fig. 2. Carrier concentration and resistivity of *p*-GaN layers at different growth pressures. The growth rate increases with enhanced growth pressure.

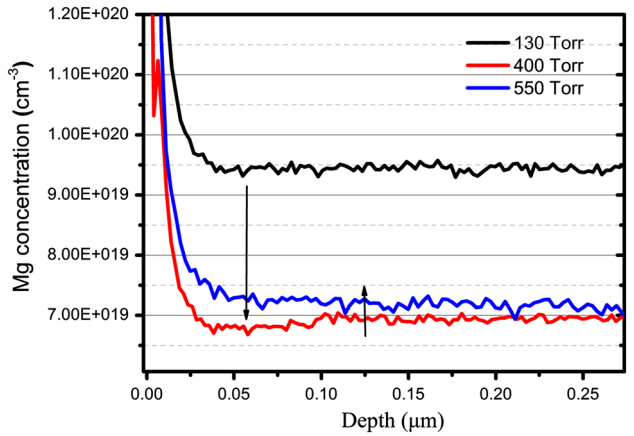

Fig. 3. Mg concentration profiles measured by SIMS for *p*-GaN layers grown under various pressures. The growth rate increases with enhanced growth pressure.

decreased growth rate at high growth pressure is ascribed to enhanced TMGa:NH_3 gas-phase adduct formation.[15] Then, we focused on the growth pressure range from 130 Torr to 400 Torr, where the growth rate changes dramatically.

The electrical properties of sample series I were measured by Hall-effect measurements, as shown in Fig. 2. With increased growth pressure, we observed increased sample resistivity and decreased hole concentration. The hole mobility increased from 6.8 cm^2/V s to 14.7 cm^2/V s. The decreased hole concentration and the increased hole mobility indicate that the increased sample resistivities are probably caused by reduced Mg incorporation efficiency. This assumption was confirmed by the SIMS data. It is shown in Fig. 3 that the Mg concentration decreased from 9.5×10^{19} cm^{-3} to 6.9×10^{19} cm^{-3} with growth pressure increasing from 130 Torr to 400 Torr. It has been proved that lowered Mg incorporation efficiency, due to enhanced parasitic reaction with increased growth pressure, may lead to the

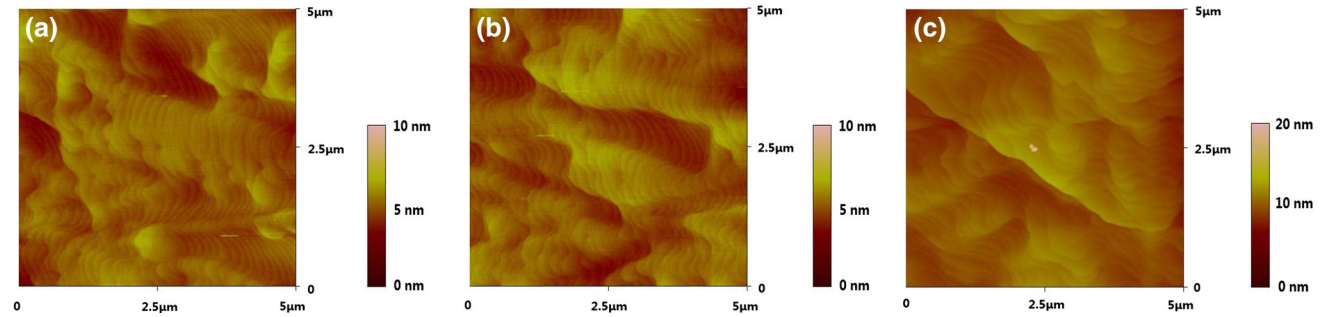

Fig. 4. AFM 5 μm $\times$ 5 μm scans of samples grown at (a) 230 Torr, (b) 300 Torr, and (c) 400 Torr in series I.

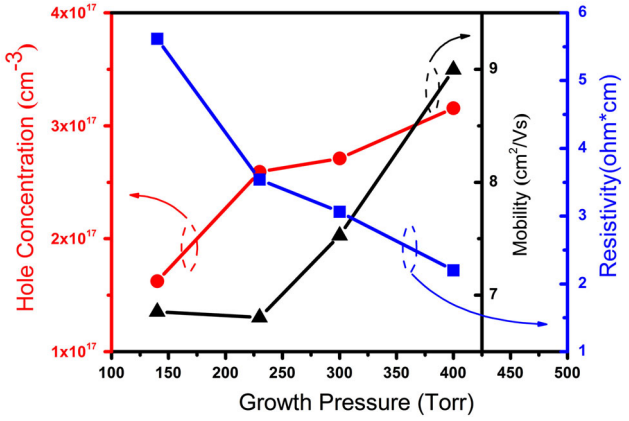

Fig. 5. Carrier concentration and resistivity of *p*-GaN layers at different growth pressures with the same growth rate.

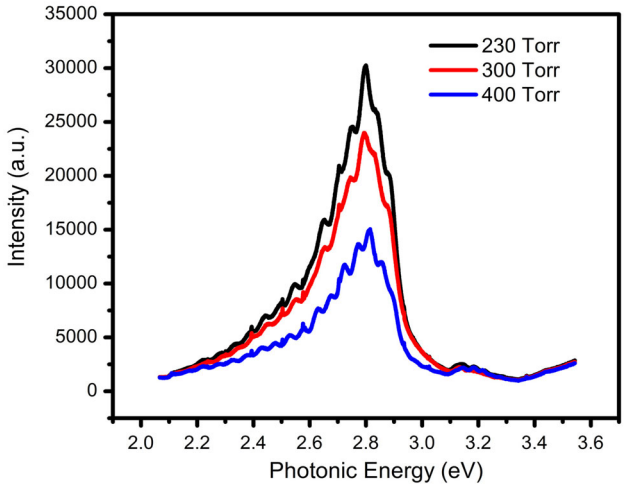

Fig. 6. PL spectra of *p*-type GaN layers grown at 230 Torr, 300 Torr, and 400 Torr in series II.

above-described phenomenon.[12,16] Then, we examined the Mg concentration of samples grown at higher pressures. If the reduction of Mg concentration is caused mainly by enhanced parasitic reaction with increased growth pressure, the Mg concentration may be further reduced at high growth pressures. However, when the growth pressure further reached 550 Torr, the Mg concentration in our experiment did not show any further reduction but slightly increased to 7.2×10^{19} cm^{-3}. Interestingly, this shows some kind of relation between the Mg concentration and growth rate. From 130 Torr to 400 Torr, the growth rate increased rapidly, in correspondence with the rapidly decreasing Mg concentration. When the growth pressure further reached 550 Torr, the growth rate slightly decreased and the Mg concentration of the samples increased slightly. The Mg concentration showed an inverse relationship with growth rate. The physical mechanism for the decline of the Mg incorporation efficiency at high growth rate caused by high growth pressure is not yet clear. It is known that surface adatoms do not have enough time to migrate to proper lattice sites at high growth rates.[11] We assume that the same phenomenon may apply to Mg adatoms, which would reduce the Mg incorporation efficiency. However, it has been reported that the Mg incorporation rate is independent of the growth rate for *c*-plane GaN when the growth rate is changed by varying the reactant flow rate.[12,17] However, those experiments were performed under relatively low growth pressures. Since low growth pressure will lead to an enhanced adatom mobility which enables surface adatoms to reach proper lattice sites in a relatively short time.[18]

Figure 4 shows 5 μm $\times$ 5 μm AFM images of sample series I. The samples shown in Fig. 4a, b, and c were prepared at growth pressures of 230 Torr, 300 Torr, and 400 Torr, respectively. The root-mean-square (RMS) roughness of the sample surfaces in Fig. 4a, b, and c was 0.612 nm, 0.659 nm, and 0.993 nm, respectively. When the growth pressure was varied between 230 Torr and 300 Torr, the RMS roughness changed little, matching very well with the tendency of the growth rate and hole concentration. When the growth pressure was varied from 300 Torr to 400 Torr, the growth rate increased rapidly. Large hills and valleys began to appear on the surface of the *p*-type layer grown under growth pressure of 400 Torr. The surface morphology of GaN epitaxial layers is controlled by the surface adatom diffusion length, which is short under high growth rates due to the limited surface adatom diffusion time. As a result,

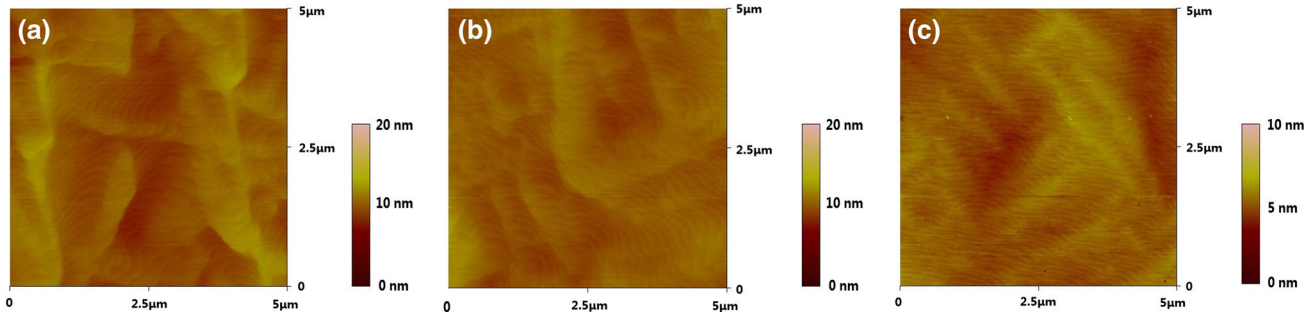

Fig. 7. AFM 5 μm $\times$ 5 μm scans of samples grown at (a) 230 Torr, (b) 300 Torr, and (c) 400 Torr in series II.

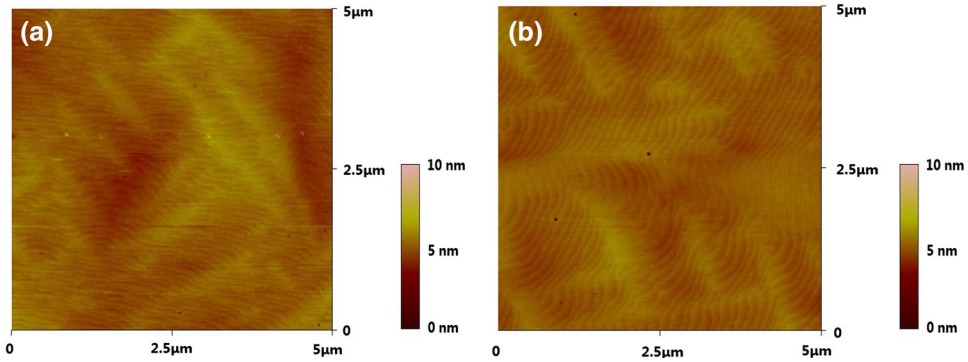

Fig. 8. AFM 5 μm $\times$ 5 μm scans of samples grown at 400 Torr with V/III ratio of (a) 16,000 and (b) 5000. The growth rates of both samples are the same.

the probability of reactant adatoms attaching to the edge of an existing terrace is limited and the step flow growth mode is inhibited, leading to a rough surface morphology. Rough surface morphology under high growth rates has also been reported by Lee et al.[11]

To eliminate the influence of the increased growth rate, we prepared another series of samples named series II. In this series, we kept the growth rate for the samples at a relatively low value of 0.4 μm/h. The Hall results are shown in Fig. 5. Interestingly, the hole concentration and resistivity show very different pressure dependence compared with series I. The hole concentration keeps increasing and the resistivity keeps decreasing with increased growth pressure. The hole mobility increased from 6.8 cm^{-3}/V s to 9.0 cm^{-3}/V s as the growth pressure increased. As shown by the SIMS data, the Mg concentration did not show any reduction with increased growth pressure in series II, which also supports the relation between the Mg concentration and growth rate described above. The improved electrical quality of the *p*-type layers may be induced by the reduction of donor-like defects. Reduction of donor-like defects will lead to an increase of the hole concentration and eliminate defect scattering, resulting in higher carrier mobilities. RT-PL measurements were carried out to further study the compensation effect in these samples. To illustrate the elimination of compensation effects, the PL spectra of *p*-GaN layers in series II are shown in Fig. 6. All samples showed a broad emission band around 2.8 eV. The intensity of this band decreased with increased growth pressure. It has been widely accepted that this band can be ascribed to donor–acceptor (D–A) recombination between an Mg_{Ga} acceptor and a deep donor associated with a nitrogen vacancy, V_N.[19] The decrease of the 2.8-eV emission band intensity implies a reduction of compensation centers associated with V_N. Such reduction of nitrogen vacancies may be ascribed to the higher NH_3 overpressure under relatively high growth pressures.[12,16]

The improved crystal quality under relatively high growth pressures in series II is also illustrated by the AFM results in Fig. 7. The samples shown in Fig. 7a, b, and c were prepared at growth pressures of 230 Torr, 300 Torr, and 400 Torr, respectively. The RMS roughness of the sample surfaces in Fig. 7a, b, and c was 0.652 nm, 0.585 nm, and 0.439 nm, respectively. The surface morphologies of series II differ greatly from series I. The *p*-type layer grown under 230 Torr shows more curved steps, and small hills are shown in those samples in series I. However, with increased growth pressure, the curved surface steps stretch out, and the hills also flatten. As a result, under 400 Torr and 0.4 μm/h, Fig. 7c shows a relatively flat surface and good step flow growth mode of the *p*-type layer. This phenomenon can also be ascribed to the increased NH_3 overpressure, as it has been proved that an

increased NH_3 overpressure can promote the step flow growth mode and thus a flattened surface.[20]

Moreover, to maintain a constant growth rate under different growth pressures, the V/III ratio was also increased with the growth pressure in series II, which may also have contributed to the enhanced NH_3 overpressure. We prepared another sample under 400 Torr and 0.4 μm/h but with a reduced V/III ratio of 5000 so as to illustrate this problem. AFM images of the samples with and without the reduced V/III ratio are shown in Fig. 8, from which it can be seen that both high-pressure samples show a flat surface and good step flow growth mode. This means that a flat surface can be realized by the high growth pressure itself.

CONCLUSIONS

The joint effect of growth pressure and growth rate on the electrical and structural quality of *p*-type GaN layers was investigated in this work. We found that the growth rate keeps increasing with the growth pressure, which leads to decreased structural and electrical properties of the *p*-type layer. With a constant growth rate, increased growth pressure results in *p*-type layers with a flat surface and relatively high hole concentration. Thus, it is assumed that enhanced NH_3 overpressure at high growth pressure may be responsible for this phenomenon.

ACKNOWLEDGEMENTS

This research was supported by the National High Technology Research and Development Program of China No. 2011AA03A105 and the State Key Development Program of Basic Research of China No. 2011CB301902.

REFERENCES

1. K. Kumakura, T. Makimoto, and N. Kobayashi, *J. Appl. Phys.* 93, 3370 (2003).
2. R.M. Lin, S.F. Yu, S.J. Chang, T.H. Chiang, S.P. Chang, and C.H. Chen, *Appl. Phys. Lett.* 101, 081120 (2012).
3. M.L. Nakarmi, K.H. Kim, J. Li, J.Y. Lin, and H.X. Jiang, *Appl. Phys. Lett.* 82, 3041 (2003).
4. H. Wang, J. Liu, N. Niu, G. Shen, and S. Zhang, *J. Cryst. Growth* 304, 7 (2007).
5. C. Simbrunner, M. Wegscheider, M. Quast, T. Li, A. Navarro-Quezada, H. Sitter, A. Bonanni, and R. Jakiela, *Appl. Phys. Lett.* 90, 142108 (2007).
6. A.Y. Polyakov, N.B. Smirnov, A.V. Govorkov, A.M. Dabiran, A.V. Osinsky, and S.J. Pearton, *Appl. Phys. Lett.* 89, 112127 (2006).
7. L. Yi-Jung, T. Tsung-Yuan, Y. Chih-Hung, C. Li-Yang, T. Tsung-Han, and L. Wen-Chau, *J. Quantum Electron.* 46, 492 (2010).
8. C.-R. Lee, J.-Y. Leem, S.-K. Noh, S.-E. Park, J.-I. Lee, C.-S. Kim, S.-J. Son, and K.-Y. Leem, *J. Cryst. Growth* 193, 300 (1998).
9. B. Schineller, A. Guttzeit, P.H. Lim, M. Schwambera, K. Heime, O. Schön, and M. Heuken, *J. Cryst. Growth* 195, 274 (1998).
10. H. Tokunaga, A. Ubukata, Y. Yano, A. Yamaguchi, N. Akutsu, T. Yamasaki, and K. Matsumoto, *J. Cryst. Growth* 272, 348 (2004).
11. W. Lee, J. Limb, J.-H. Ryou, D. Yoo, T. Chung, and R. Dupuis, *J. Electron. Mater.* 35, 587 (2006).
12. P. Kozodoy, S. Keller, S.P. DenBaars, and U.K. Mishra, *J. Cryst. Growth* 195, 265 (1998).
13. W.G. Breiland, M.E. Coltrin, J.R. Creighton, H.Q. Hou, H.K. Moffat, and J.Y. Tsao, *Mater. Sci. Eng. R* 24, 241 (1999).
14. B. Mitrovic, A. Gurary, and L. Kadinski, *J. Cryst. Growth* 287, 656 (2006).
15. M. Dauelsberg, C. Martin, H. Protzmann, A.R. Boyd, E.J. Thrush, J. Käppeler, M. Heuken, R.A. Talalaev, E.V. Yakovlev, and A.V. Kondratyev, *J. Cryst. Growth* 298, 418 (2007).
16. Y.L. Xian, S.J. Huang, Z.Y. Zheng, B.F. Fan, Z.S. Wu, H. Jiang, and G. Wang, *J. Cryst. Growth* 325, 32 (2011).
17. A. Chakraborty, H. Xing, M.D. Craven, S. Keller, T. Mates, J.S. Speck, S.P. DenBaars, and U.K. Mishra, *J. Appl. Phys.* 96, 4494 (2004).
18. S.M. Ko, J.H. Kim, Y.H. Ko, Y.H. Chang, Y.H. Kim, J. Yoon, J.Y. Lee, and Y.H. Cho, *Cryst. Growth Des.* 12, 3838 (2012).
19. U. Kaufmann, M. Kunzer, M. Maier, H. Obloh, A. Ramakrishnan, B. Santic, and P. Schlotter, *Appl. Phys. Lett.* 72, 1326 (1998).
20. C. Ratsch, J. Garcia, and R.E. Caflisch, *Appl. Phys. Lett.* 87, 141901 (2005).